

# Imaging of photothermal tissue expansion via phase sensitive Optical Coherence Tomography

Hendrik Spahr<sup>a</sup>, Linda Rudolph<sup>a</sup>, Heike Müller<sup>a</sup>, Reginald Birngruber<sup>a,b</sup>, and Gereon Hüttmann<sup>a,b</sup>

<sup>a</sup>University of Lübeck, Institute of Biomedical Optics, Peter-Monnik-Weg 4, Lübeck, Germany

<sup>b</sup>Medical Laser Center Lübeck GmbH, Peter-Monnik-Weg 4, Lübeck, Germany

## ABSTRACT

Phase sensitive OCT enables the measurement of thermal expansion in laser irradiated material at high lateral and temporal resolution. In principle, a calculation of the 3D temperature distribution and its temporal evolution should be possible by evaluating the local expansion. This could be utilized for a non-invasive and very fast temperature measurement, e.g. to realize an online dosimetry for photocoagulation. The possibilities of quantitative investigations at high axial and lateral resolution are demonstrated by imaging the reversible thermal expansion in laser irradiated multilayer silicone phantoms.

**Keywords:** Optical Coherence Tomography, Doppler, phase sensitive, photothermal, temperature

## 1. INTRODUCTION

Phase sensitive Optical Coherence Tomography enables the measurement of small morphologic changes at high spatial and temporal resolution.<sup>1</sup> Besides the imaging of fluidal dynamics,<sup>1-3</sup> a possibly important clinical application of this technique has been developed recently and is subject of current scientific research: The temperature distribution and retinal tissue changes during photocoagulation treatment are investigated via phase sensitive OCT.<sup>5</sup> During photocoagulation the temperature typically rises by about 30 to 50 K; but it turned out, that even much smaller heatings already induce a clearly measurable phase shift. This effect could be utilized for a non-invasive measurement of temperature distributions in any semitransparent media. A similar way to determine absorber concentrations in turbid media has been reported just recently.<sup>4</sup> It is as well capable of spatially resolved investigations by analysing the thermal response to modulated irradiation. But until now no other photothermal OCT based method has been demonstrated to investigate the temporal evolution of an arbitrary temperature distribution. This new principle is evaluated by determining the temperature distribution in laser irradiated multilayer silicone phantoms. The results can be compared to numerical simulations to verify its accuracy.

## 2. THEORY

In most solids and fluids the temperature increase caused by the absorption of light yields an increase of the volume. This effect is called (photo)thermal expansion and it is usually quantified by the linear and volumetric expansion coefficients  $\kappa$  or  $\gamma$ , respectively.

$$\frac{\partial L}{\partial T} = \kappa L \quad \text{and} \quad \frac{\partial V}{\partial T} = \gamma V \quad (1)$$

The process of photothermal expansion has to satisfy the conservation of mass. The local temperature increase  $\Delta T$  yields an increasing pressure  $p$ , which is almost instantaneously converted into an increase of the volume  $V$  (because of the low compressibility of solids and liquids). If the same mass  $m$  fills a larger volume  $V$ , the density  $\rho = \frac{m}{V}$  of the heated material decreased. In fluid dynamics the conservation of mass is described by the so called equation of continuity:

$$\frac{\partial \rho}{\partial t} + \text{div}(\rho \vec{v}) = 0 \quad (2)$$

with the velocity vector field  $\vec{v}$ . This can be transformed into:

$$\frac{\partial \rho}{\partial V} \cdot \frac{\partial V}{\partial T} \cdot \frac{\partial T}{\partial t} + \text{div}(\rho \vec{v}) = 0. \quad (3)$$

By using

$$\frac{\partial V}{\partial T} = \gamma \cdot V \quad \text{and} \quad \frac{\partial \rho}{\partial V} = \frac{-m}{V^2} \quad (4)$$

this yields

$$-\gamma \cdot \frac{\partial T}{\partial t} + \text{div}(\vec{v}) \approx 0. \quad (5)$$

Integrating over time  $t$  we get

$$\Delta T \approx \frac{\text{div}(\Delta \vec{r})}{\gamma} \quad (6)$$

So a local increase of the temperature yields a divergence of the displacement vector field  $\Delta \vec{r}$ :

$$\text{div}(\Delta \vec{r}) = \frac{\partial \Delta x}{\partial x} + \frac{\partial \Delta y}{\partial y} + \frac{\partial \Delta z}{\partial z} \quad (7)$$

This divergence only depends on the temperature and the thermal expansion coefficient. In phase sensitive OCT the phase shift  $\Delta \phi$  provides information about the longitudinal displacement  $\Delta z$ . The unwrapped phase data  $\Delta \Phi_i$  can be converted to the corresponding changes in optical path length, which is twice the longitudinal displacement  $\Delta z_i$  times the index of refraction  $n$ . So the longitudinal displacement (in optical pathlength) between two successive frames  $i - 1$  and  $i$  is given by:

$$\Delta z_i = \Delta \phi_i \cdot \frac{\lambda_0}{4\pi} \quad (8)$$

Summing up the displacements  $\Delta z_i$  between successive frames in the measured series of B-scans, one finally gets the evolution of the longitudinal displacement  $\Delta z$  for each pixel of the B-scan. As long as just this component of the local displacement is known, some further assumptions regarding the symmetry of the problem have to be made to estimate the local divergence. The simplest case is a multilayered structure that is homogeneously irradiated, so the physics are completely independent on the in-plane-coordinates  $x$  and  $y$ . Then the expansion is simply given by the last term of the above equation 7. In spherically symmetric problems, e.g. in the case of a sufficiently small absorber localized in a homogeneous and isotropic environment, one can place the origin of the coordinate system into the center of symmetry. The measured displacement vector field has to be corrected by adding the right  $x$ -component to satisfy spherical symmetry without changing the  $z$ -component (see Fig.1):

$$\Delta x_i = \Delta z_i \cdot \frac{x}{z} \quad (9)$$

Hence, whenever planar or radial symmetry can be assumed, an estimation of the local displacement is possible, which allows to estimate the time resolved evolution of a 3D temperature distribution within the sample. In the case of retinal tissue this is either the case if the irradiation is sufficiently homogeneous or if the radiation spot on the retinal pigment epithelium is small compared to the thickness of the scattering neuronal layers. Once the local displacement is known, the expansion can be calculated straight forward as the divergence of this 3D vector field.

### 3. EXPERIMENTAL SETUP

Multilayered silicone phantoms were prepared, whose optical properties have been custom tailored by adding absorbing and scattering pigments to the highly transparent base material. The individual layers of a multilayered silicone phantom were prepared one after the other. Cover slips served as spacers as well as delimiters to create layers of 160  $\mu\text{m}$  thickness each. Air inclusions and micro bubbles were removed by the vacuum of a desiccator to obtain homogeneous optical properties. The phantoms were irradiated using a ZEISS Visulas 532s at a wavelength of 532 nm with a laser power of 50 to 1500 mW. The spotsize was chosen to be 2 mm in diameter.

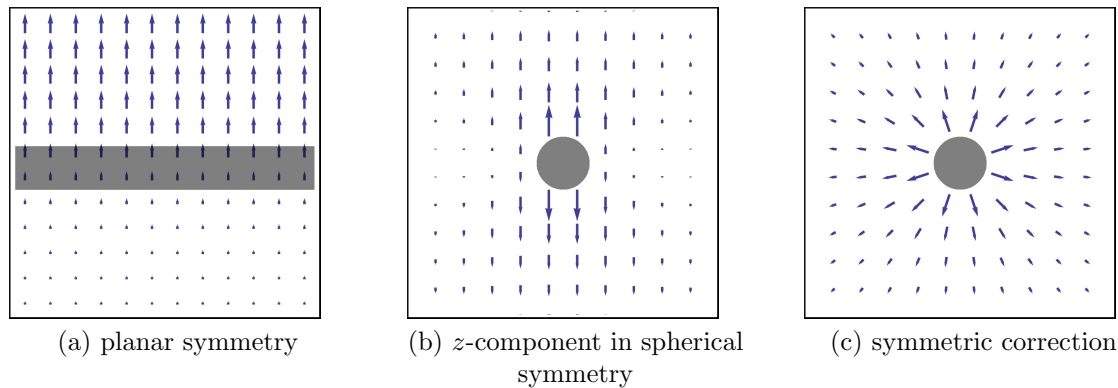


Figure 1. (a) In planar symmetry displacements will only occur in longitudinal direction, so the measured signal does not have to be corrected. (b) In spherically symmetric systems the phase shift is just an indication for the longitudinal  $z$ -component. It has to be corrected to fulfill spherical symmetry without changing the  $z$ -component (c).

Doppler OCT measurements of these laser irradiated phantoms were realized by a commercially available high speed Fourier domain OCT system (Hyperion Spectral Radar, Thorlabs GmbH, München, Germany), whose line detector (Basler Sprint SpL 4096 140km) is capable of reading 1024 pixels at a rate of 200 kHz. The center wavelength of the external 20 mW super luminescence diode is located at 842 nm with an FWHM bandwidth of 50 nm. The irradiation laser and the OCT beam are combined by a beam splitter and then focused into the specimen. Two galvanometric mirrors scan the OCT beam over the sample, generating B-scans with a resolution of typically 100 to 1000 A-scans, depending on the need for either high frame rate or high lateral resolution, respectively.

#### 4. DATA PROCESSING

The raw OCT spectra were streamed to disk in binary file format for subsequent offline processing and evaluation. They were offset corrected by subtracting the previously measured offset spectrum. After a numerical apodization that normalized the data to the spectral intensity of the light source, the data were dechirped into a spectrum equally spaced in the wavenumbers  $k$ , and then Fourier transformed. The absolute value of the complex Fourier coefficients of each frame can be plotted to get a scattering intensity image. In phase sensitive mode, the differences between phase values of corresponding pixels in successive B-Scans are subtracted from each other to detect small changes in optical path lengths.<sup>1</sup> The Doppler dynamic range, i.e. the range of measurable longitudinal velocities, is mainly limited by the stability of the setup, which determines the minimum resolvable velocity, and the measurement speed (in fps), which has to be sufficiently high to detect fast movements in the sample without violent phase wrapping or even fringe washout of the signal. Morphologic changes and tissue movements exceeding a velocity of  $\lambda_0/4n$  per frame result in wrapped phases that have to be unwrapped using 1D or 2D unwrapping algorithms (see Fig.2b). 1D phase unwrapping is simple and extremely fast, but only possible if the phase data is of very high quality or can be strongly averaged without losing relevant information. Otherwise, mistaken or overseen crossings of phase discontinuity lines by the integration path would corrupt the data, adding the wrong multiple of  $2\pi$  to every following pixel. A good agreement between processing time and reliability can be found in a quality guided 2D phase unwrapping algorithm that first creates a quality map assigning a quality factor to every pixel of the B-scan.<sup>7</sup> The quality factor is determined by the absolute value of the complex Fourier coefficient, i.e. the intensity of the corresponding pixel, and the local phase derivative variance. Then, starting in the area of highest quality, a quality guided flood filling algorithm unwraps the whole B-Scan. An even more stable and reliable, but also quite time consuming 2D unwrapping algorithm has been developed by Goldstein.<sup>8</sup> In a first step it scans the image for ends or beginnings of phase jump lines and marks them as positive and negative residues, that change the result of any encircling closed integration path from zero to a multiple of  $2\pi$ . In a second step, these residues are connected by so called branch cuts, that cannot be crossed by the integration path, so residues can only be encircled pairwise (if at all). The third step is the actual unwrapping process, which can now be done in arbitrary paths without changing the result, as long as

no branch cut will be crossed. This algorithm is best suited for noise corrupted data and does not depend on averaging of the original phase data.

## 5. RESULTS AND DISCUSSION

### 5.1 Imaging lateral and in-depth variations of absorbance

To demonstrate the ability of phase sensitive OCT to visualize photothermal dynamics in a depth resolved way, a multilayered silicone phantom consisting of 5 different layers (160  $\mu\text{m}$  thickness each) has been imaged while being locally irradiated. The photothermal consequences can clearly be seen in Fig.2a, where two localized spots of high (and therefore wrapped) phase shifts appear within the sample, indicating the high absorbance of the 2<sup>nd</sup> and 4<sup>th</sup> layer of the 5 layer phantom. Notice that high temperatures are not indicated by high phase shifts but by a high divergence, i.e. gradient of the phase shifts. In Fig.2b the phase sensitive OCT measurement of another phantom is shown. This one consists of a scattering layer on top of two different basements: On the left hand side the basement is transparent for the irradiation wavelength, while the absorbance of the right hand side is higher. The irradiation has nearly no effect on the transparent basement. However, the absorbing basement is heated and the thermal expansion can qualitatively be seen in the resulting phase shifts.

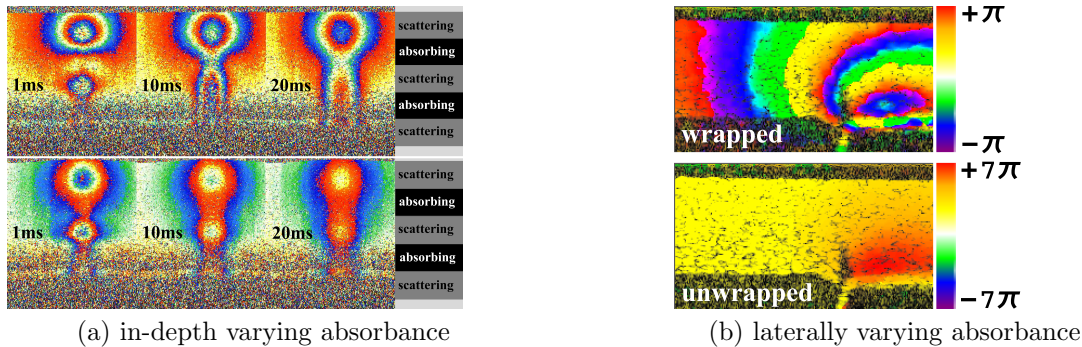


Figure 2. (a) In this multilayer phantom the high absorbance of the 2<sup>nd</sup> and 4<sup>th</sup> layer causes localized spots of high thermal expansion. The wrapped phases are colour coded from blue for a phase difference of  $-\pi$  to red for a difference of  $+\pi$ . Each frame has a width of 1 mm (250 A-scans). The images have been taken 1, 10 and 20 ms after the laser had been turned on and after the end of the irradiation, respectively. (b) The higher absorbance of the silicone basement in the right hand side of the phantom causes thermal expansion when the phantom is irradiated homogeneously.

### 5.2 Temperature distribution in layered silicone phantoms

The phase shift distribution were converted into a temperature distribution the following way:

1. unwrapping of the wrapped phase values  $\Delta\phi_i$
2. converting of the unwrapped phase values  $\Delta\Phi_i$  into changes of pathlengths  $\Delta z_i$  using equation 8
3. summing up all  $\Delta z_i$  to the total longitudinal displacement  $\Delta z$
4. symmetry considerations for an estimation of unknown components of  $\Delta\vec{r}$
5. calculation of the divergence of  $\Delta\vec{r}$
6. calculation of the temperature distribution using the thermo optical expansion coefficient and equation 6

The thermo optical expansion coefficient  $\kappa'$  mentioned in the last step combines the two thermal effects of mechanical expansion and thermal change of the refractive index into one quantity, that can be determined for any semitransparent material using phase sensitive OCT. For an evaluation this method has been applied to the multilayer phantom that can be seen in Fig.3a. It has been irradiated for 250 ms with a laser power 1 W on a

gaussian spot of 2 mm in diameter. The measured phase shift  $\Delta\phi_i$  of each frame is shown in Fig.3b and Video 1. The very few phasewraps have been unwrapped using the Goldstein algorithm to obtain the unwrapped phase values  $\Delta\Phi_i$  (see Fig.3c and Video 2) that can be converted into changes of optical pathlengths  $\Delta z_i$  between consecutive B-Scans  $i - 1$  and  $i$ . Because of the planar symmetry the  $x$ - and  $y$ -component of the displacement may assumed to be zero. The cumulative sum

$$\Delta z = \sum_{i=0}^n \Delta z_i \quad (10)$$

is the total displacement between the first and the  $n^{\text{th}}$  frame of the measurement (see Fig.4a and Video 3). The displacement distribution is dominated by global upwards movements that are free of divergence and therefore they do not provide any information about the layered structure of the phantom. The derivative in  $z$ -direction reveals the relevant information, the expansion  $\epsilon$  of the material:

$$\epsilon = \text{div}(\Delta\vec{r}) = \frac{\Delta z(z_1) - \Delta z(z_2)}{z_1 - z_2} \quad (11)$$

This way the layered structure of the phantom is revealed in the photothermal OCT measurement (see Fig.4b and Video 4). Using the photo-thermal expansion coefficient  $\kappa'$  one can now estimate the temperature distribution within the sample (Fig.4c and Video 5). In the second layer the temperature rises by about 240 K. By Monte Carlo simulations of the photon propagation in the phantom we estimated that 350 mW of the 1000 mW irradiation are absorbed in that layer. Neglecting heat conduction, this would cause a temperature increase of about 190 K after an irradiation time of 500 ms. Considering the possible inaccuracies in quantities like for example the absorption coefficient, heat capacity, and the exact beam profile this fits quite well to the experimental data.

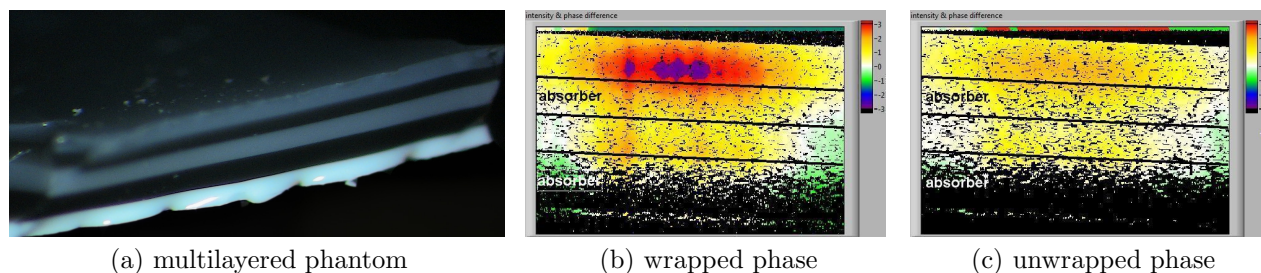


Figure 3. (a) This multilayer phantom has high absorbances of 22 and 87  $\text{cm}^{-1}$  in the 2<sup>nd</sup> and 4<sup>th</sup> layer, respectively. So these layers are expected to heat up when the laser irradiation starts. (b) VIDEO 1 The wrapped phases are colour coded from blue for a phase difference of  $-\pi$  to red for a difference of  $+\pi$ . Each frame has a width of 2 mm (250 A-scans). Phase wraps occur in the first layer, which does not necessarily mean that the highest temperatures can be found in that layer <http://dx.doi.org/10.1117/12.911429.1> (c) VIDEO 2 The phase values have been unwrapped using the Goldstein algorithm <http://dx.doi.org/10.1117/12.911429.2>

## 6. CONCLUSION

High speed Doppler OCT is a sensitive tool to image photothermal dynamics in any semitransparent media. The possibilities of quantitative investigations with high axial and lateral resolution have been demonstrated by imaging the reversible thermal expansion in laser irradiated bilayer and multilayer silicone phantoms. Irradiation of phantoms with laterally or in-depth varying absorbance caused an accordingly varying phase shift, that already gives a qualitative idea of the local absorbance. The conversion of this phase shift distribution into a 3D displacement vector field first of all requires a removal of the  $2\pi$  ambiguity of the wrapped phases. This can be done by different unwrapping algorithms. The final conversion into local expansions is somehow difficult due to the fact that just one (the longitudinal) component of the 3D displacement vector field is known. Without serious modifications of the measurement setup, this problem can only be solved if certain symmetries can be assumed. In planar or spherical symmetric systems the divergence of the displacement vector field and therefore

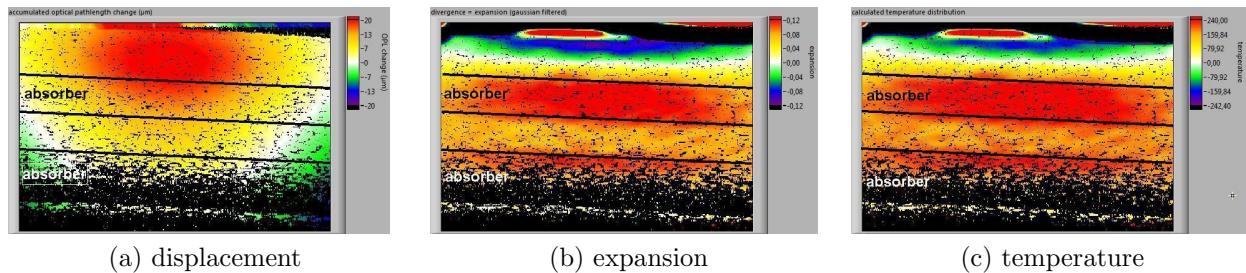


Figure 4. (a) VIDEO 3 The displacement distribution is dominated by global upwards movements that are free of divergence and therefore do not provide any information about the layered structure of the phantom <http://dx.doi.org/10.1117/12.911429.3> (b) VIDEO 4 The derivative in  $z$ -direction reveals the relevant information, the expansion  $\epsilon$  of the material <http://dx.doi.org/10.1117/12.911429.4> (c) VIDEO 5 The local temperature can be calculated, if the thermo optical expansion coefficient is known <http://dx.doi.org/10.1117/12.911429.5>

the expansion of the material can be estimated knowing just the  $z$ -component of the displacement. Hence, in such systems a quantitative analysis of the temperature distribution and its temporal evolution is possible. This has been shown for a laser irradiated multilayer silicone phantom.

### ACKNOWLEDGMENTS

This project was funded by TANDEM (Center for Technology and Engineering in Medicine) of University and Polytechnic of Lübeck and the Ministry of Economics and Science in Schleswig-Holstein. Thanks to Dierck Hillmann from Thorlabs HL AG for excellent technical support.

### REFERENCES

- [1] Drexler, W. Fujimoto, J.G.(Eds.): [Optical Coherence Tomography, Technology and Applications], Springer (2008)
- [2] Yazdanvar, S. Rollins, A.M Izatt, J.A. "Imaging and velocimetry of the human retinal circulation with color Doppler optical coherence tomography" *Opt. Lett.* 25, 1448 (2000)
- [3] Leitgeb, R.A. Schmetterer, L. Drexler, W. Fercher, A.F. Zawadzki, R.J. Bajraszewski, T. "Real-time assessment of retinal blood flow with ultrafast acquisition by color Doppler Fourier domain optical coherence tomography," *Opt. Express* 11, 3116-3121 (2003)
- [4] G. Guan, R. Reif, Z. Huang, R.K. Wang, "Depth profiling of photothermal compound concentrations using phase sensitive optical coherence tomography", *Journal of Biomedical Optics* 16, Issue 12, pp. 126003-126003-9 (2011)
- [5] Miller, H.H. Ptaszynski, L. Schlott, K. Bonin, T. Bever, M. Koinzer, S. Birngruber, R. Brinkmann, R. and Httmann, G., "High speed OCT imaging of temperature distribution and retinal tissue changes during photocoagulation" *Proc. SPIE* 7889, 78890E (2011)
- [6] White, B. Pierce, M. Nassif, N. Cense, B. Park, B. Tearney, G. Bouma, B. Chen, T. and de Boer, J. "In vivo dynamic human retinal blood flow imaging using ultra-high-speed spectral domain optical coherence tomography," *Opt. Express* 11, 3490-3497 (2003)
- [7] Pritt, M.D. "Phase unwrapping by means of multigrid techniques for interferometric SAR" *IEEE Transaction on Geoscience and Remote Sensing* 34, No. 3, pp. 728-738 (1996)
- [8] Goldstein, R.M. Zebker, H.A. Werner, C.L. "Satellite radar interferometry: two-dimensional phase unwrapping" *Radio Science* 23, No. 4, pp.713-720 (1988)